

Electrical Properties of a Magnetic Brush Using a High Resolution Field Probe

Michael D. Thompson, Paul W. Morehouse, Palghat Ramesh, John G. Shaw Xerox Research Center Webster, Webster NY 14580 USA
 Helena Silva University of Connecticut, Electrical & Computer Engineering Storrs, CT 06269-2157 USA

Abstract

Dry powder xerographic marking systems are capable of high quality printing but there is still need to improve their capabilities to better compete in offset markets. Many of these systems use two component magnetic brush technology to develop latent electrostatic images. The electrical properties of the developer material which makes up the magnetic brush play a large role in the quality of the developed image. Our desire to improve image quality characteristics affected by development has led us to explore the magnetic brush in more detail.

We have used a high resolution electric field probe to characterize the dielectric constant and conductivity of a two component developer in a magnetic brush. Standard techniques use large area cells which look at the integrated properties of the developer material and cannot resolve variations at the spatial scales that are relevant for image uniformity. Magnetic brush structure is likely to translate into local electric field variation during the development process producing variations in toned image density on the photoreceptor and ultimately in the final printed image. Variations in electrical properties due to position in the development zone and magnetic field are looked at and discussed in the context of image quality. Realistic particle simulations are compared to experimental data.

Introduction

Magnetic Brush Development has been successfully used in high quality xerographic printers for many years and, in some form, is the main technology used today in these systems. Continual improvement of magnetic brush and materials has enabled very high quality printing but some deficiencies relative to offset lithographic printing remain, some which can be attributed to properties of the magnetic brush itself. In particular, image noise can be produced which adds to graininess of xerographic prints as illustrated in figure 1. This problem gets worse if the magnetic brush structure size approaches or is larger than the halftone dot size. High resolution printing with high frequency halftone screens is especially susceptible to this contribution to image noise.

When developer is loaded on the magnetic developer roll to form a magnetic brush, the carrier beads, surrounded by toner particles, form "stalagmite" -like structures. This geometry results in a non-homogeneous brush structure with more and less dense areas which are expected to result in variations in the local development electric field as well as affecting local toner supply. Because these structures magnetically repel each other, some structure persists even when the material is compressed in the development zone and can increase if the bead chains gain charge during the development process exacerbating the noise in the final printed image. We have observed this structure in the magnetic

brush to persist over times longer than the times spent by an image in the development zone.



Figure 1 Illustration of magnetic brush structure and high frequency noise in a halftoned image.

Theory

For magnetic brush systems, the developed mass per unit area (M/A) can be related to the applied voltage (V) by

$$\frac{M}{A} = \frac{\epsilon_0 V}{\left(\frac{q}{m}\right) \left(\frac{t_p}{K} + \frac{\Lambda}{v} \right)} \quad (1)$$

(see for example Schien [1]) where Λ is the effective dielectric thickness of the developer brush and v is the speed ratio between the developer roll and receiver. Λ is defined as the ratio of the distance of the effective developer electrode from the receiver and the effective dielectric constant of the developer brush. The location of the effective electrode in the developer brush depends on the conductivity of the brush. For an insulative developer, the effective electrode is located at the surface of the developer roll, while in the conductive case, the effective electrode is located near the tips of the brush. Semi-conductive brushes may be treated using a cross over function between the insulative and conductive limits and the effective electrode lies somewhere within the developer brush itself [2]. The conductivity and effective dielectric constant we use to characterize the brush are strong functions of the structure and flow of developer material. Nonuniformities in structure and flow of the developer brush can lead to local fluctuations in the conductivity and dielectric constant of the brush. These fluctuations in the developer electrical properties can modulate the local electric field at the tips of the developer brush which in turn can cause variations in developed mass in a solid area image (solid area mottle) or variations in the size of developed halftone dots (halftone graininess).

Experiments

A high resolution field probe was constructed to characterize the fluctuations in the dielectric constant and conductivity of a magnetic brush. Previous measurements [3] have used large area cells to give information on the integrated properties of the brush and cannot resolve variations in the spatial scales that are relevant for graininess and mottle (sub-mm and above). The ability to resolve this structure using the field probe is critical to a better understanding of image noise root causes.

The high resolution probe is made of a 75 μm diameter copper magnet wire imbedded in solder and polished flush to a brass plate. It is covered by a 30 μm film made from a photoreceptor transport layer.

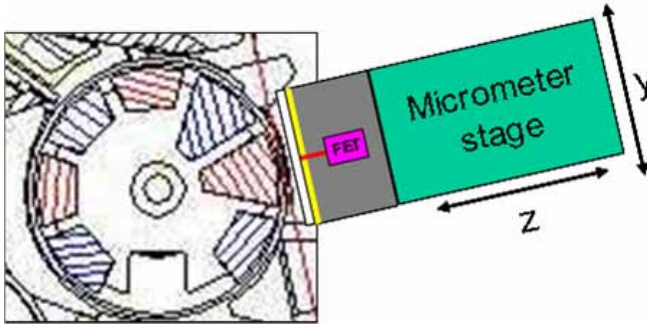


Figure 2 Schematic of the high resolution field probe.

The probe is connected to a charge sensitive inverting amplifier with a sensitivity of 0.19 mV/(V/ μm) with a flat frequency response from 2Hz to 100KHz. The transport layer is used to simulate the development conditions in an actual printer, where the magnetic brush is in contact with a photoreceptor. Schematics of the probe geometry and circuit are shown in Figures 2 and 3 respectively. In these experiments we are using a magnetic brush development system from a high speed printer to allow us to look at ranges of magnetic fields, toner concentrations and

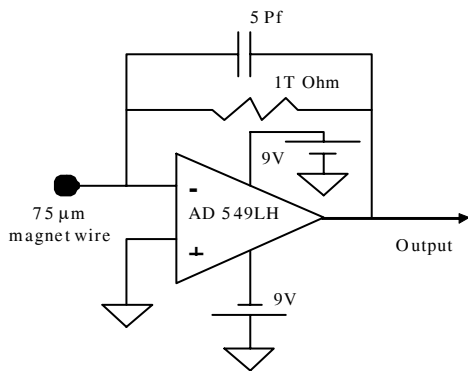


Figure 3 High resolution probe circuit schematic

developer packing typically found in practice. The probe is mounted on a stage with x-y-z micro-positioning capability that allows the mapping of the electric field at the surface of the transport layer for different developer thickness (gap between the magnetic roll and the transport layer) and different points along the development zone. In operation, the probe substrate is grounded

and a high voltage pulse (500 μs) is applied to the magnetic roll. The probe signal records the induced charge. A typical response signal is shown in Figure 4.

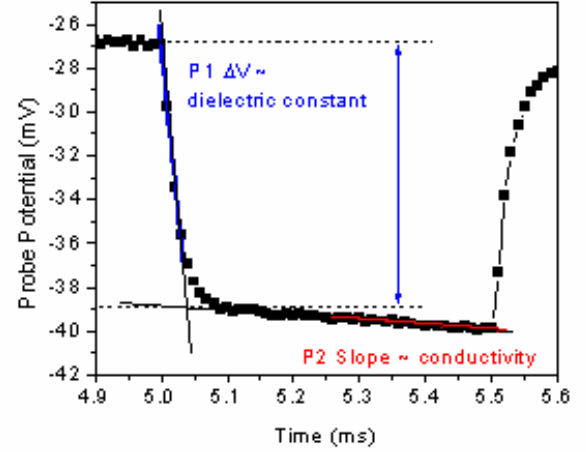


Figure 4 Typical probe signal when a high positive voltage pulse is applied to the magnetic roll. The initial voltage drop and the subsequent slope are related to the magnetic brush dielectric constant and conductivity, respectively.

The probe signal is directly related to the electric field at the surface of the transport layer. The initial fast response $\sigma_s^d(t=0)$ is due to capacitive coupling and depends on the dielectric constant of the magnetic brush. After the initial fast transient charge can flow through the brush, the change in voltage ($d\sigma_s^d/dt$) then depends on the effective conductivity of the brush (see Fig. 4). From this data, the dielectric constant and the conductivity of the developer can be extracted using Eqs. 2 and 3 where k_d and t_d are the magnetic brush dielectric constant and thickness, k_p and t_p are the dielectric constant and thickness of the transport layer. σ_s^d is the probe voltage (directly related to the surface charge at the probe - photoreceptor interface) with developer present and σ_s^{air} is the probe signal with no developer present.

$$k_d = \frac{t_d \frac{\sigma_s^d(t=0)}{\sigma_s^{air}}}{t_d + \frac{t_p}{k_p} - \frac{t_p}{k_p} \frac{\sigma_s^d(t=0)}{\sigma_s^{air}}} \quad (2)$$

$$\gamma_d = \left. \frac{d\sigma_s^d}{dt} \right|_{t=0} \frac{t_d + \frac{t_p}{k_p}}{k_d \epsilon_0 \frac{t_d}{k_d}} \quad (3)$$

In order to study the variations of the electrical properties of the developer as seen by a latent image, we allow the brush to reform and repeat the measurements 100 times after advancing the magnetic roll by approximately 130 μm (figure 5). The variations in signal are due to the structure of the magnetic brush and the finite size of the probe. Although the diameter of our probe (75 μm) is large relative to the diameter of our carrier beads (35 μm), physical structure we see in both the brush and the developed image is larger scale than either of these and the magnitude of the noise levels we see in the signal should correlate to the noise we see in the developed and final printed image. The measurements are done for different pulse voltages, different positions in the zone (which are at different magnetic fields and different developer material packing fraction) and two different magnetic field configurations.

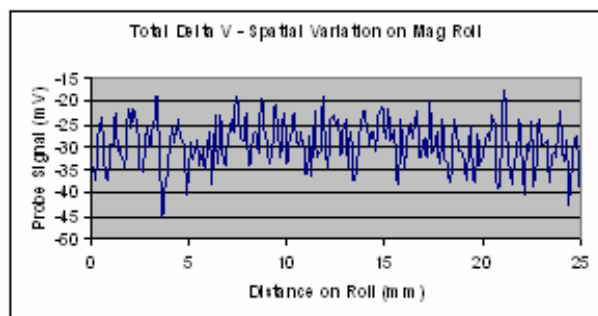


Figure 5 Spatial variation of probe signal initial voltage drop that relates directly to dielectric constant. Variations along the brush are due to the complex structure of the magnetic brush.

Results

The static DC results show that the dielectric constant and the conductivity of the material vary across the development zone.

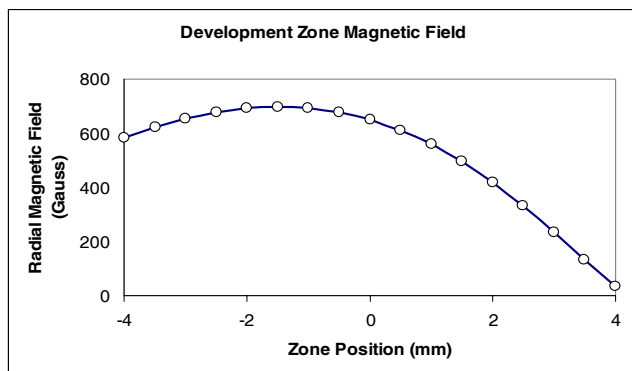


Figure 6 Radial magnetic field map through the nip at center of development gap.

Figure 6 shows the bare radial magnetic field which mediates development as we sweep along the development zone in the print process direction. Note from the figure the maximum radial field occurs just before the minimum gap in the development zone which is at 0. The values for dielectric constant change only

slightly for different pulse voltages (figure 7) unlike the conductivity which is strongly dependent on the electric field (figure 8). At 300 V, the maximum dielectric constant is approximately 4.8 and the maximum conductivity is approximately $1.5 \times 10^{-10} (\Omega \cdot \text{cm})^{-1}$.

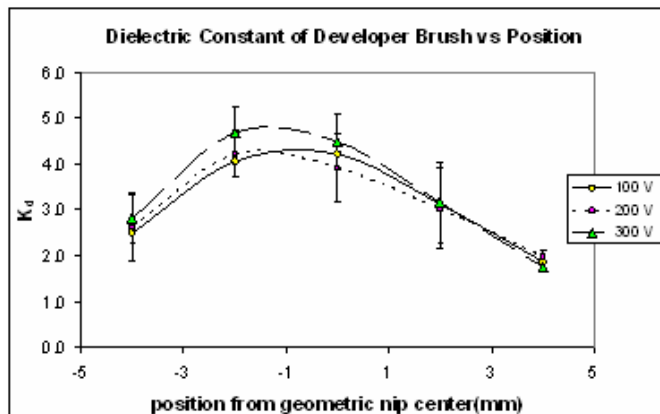


Figure 7 Dielectric constant map through the development nip. Note maximum occurs near peak radial magnetic field and is relatively independent of the electric field. Pulse voltages are 100, 200 and 300V.

The maximum values correspond to the highest radial magnetic field component which is approximately at -2 mm from the geometrical nip center. This also corresponds to the lowest relative variations (standard deviation over the 100 measurements at each voltage and zone location) in these properties as the brush reforms each time. The largest relative variations happen at the exit of the zone which may be critical since it is the last part of development seen by a latent image on the photoreceptor. The relative dielectric constant standard deviation (standard deviation of repeated measurements after the brush reforms divided by the average dielectric constant) is around 30% at the exit of the zone and the relative conductivity standard deviation, defined in the same way, is above 100% at the exit of the zone. These large fluctuations in electrical properties as the brush reforms can have a significant effect on the fields across the developer and at the photoreceptor surface which control the development process.

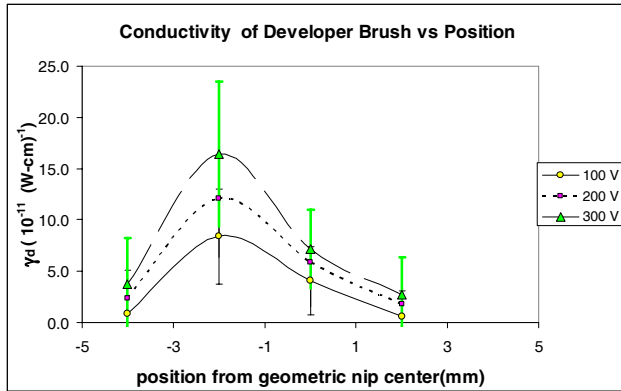


Figure 8 Developer conductivity map through the development nip. Note the strong electric field dependence. Pulse voltages are 100, 200 and 300V.

As an example to look at the effect of brush electrical property fluctuations on image noise a set of experiments was performed involving modification of the magnetic field in such a way as to reduce the physical structure of the magnetic brush. We use magnetic configuration “A” which is a standard configuration and magnetic configuration “B” which has reduced physical structure. Mapping the dielectric constant of developer across the development zone was not revealing but the variation in the conductivity for the two magnetic configurations using a 200V pulse shows a marked difference between the two. Configuration “B” shows significantly lower noise in the conductivity measurement than configuration “A” for the same developer material (figure 9). Results for image noise for the two magnetic configurations are shown in figure 10. A corresponding lowering of the high frequency noise is shown.

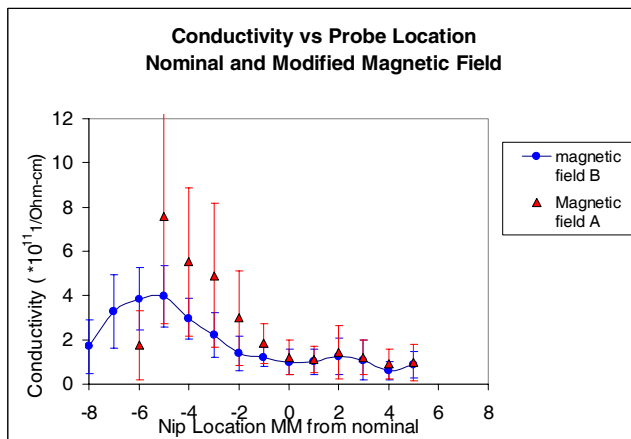


Figure 9 Developer conductivity map for two magnetic configurations A and B showing noise in both measurements. The conductivity range is smaller than the previous measurements in figs 7 and 8 because of toner concentration and geometry differences.

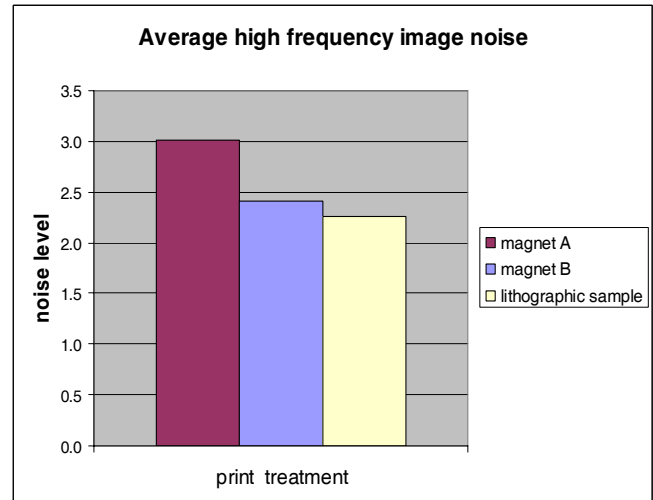


Figure 10 Example of high frequency image noise in final xerographic print compared to same print using original magnet configuration and compared to a lithographic print of the same target.

Simulations

Continuum models which have been used historically [4] attempt to characterize the properties of the magnetic brush in an average way to describe macroscopic behavior of the xerographic development process. When trying to understand details of magnetic brush development it is important to understand how parameters such as particle properties or geometry influence the development process. This understanding will enable us to predict behavior of the system when fundamental changes are made to materials as well as help guide decisions to bring about desired changes in the process.

To this end we are developing a tool within the Xerox Particle Simulation Environment (XPSE) [5,6] which is being used to model and study the magnetic brush at a fundamental level. Realistic interactions between the particles and three-dimensional physical objects enable prediction of macroscopic behaviors from microscopic particle-force models. This simulation environment includes electrostatic and magnetic interactions as well as detailed particle-particle interactions to give a detailed picture of magnetic brush behavior. The simulation also includes carrier bead-bead non-linear conduction, imposed toner q/m and particle size distributions as well as a model of a particle-particle and particle photoconductor adhesion forces. Figure 11 shows a small cell used to simulate electrical measurements similar to those made with the field probe. Numerical experiments were performed using a random starting seed for each run to simulate reformation of the magnetic brush for each measurement. A voltage pulse is applied across the cell and the charge density at the tips of the brush vs time is recorded. The simulation gives distributions of dielectric constant and conductivities for the magnetic brush similar to the field probe experiments, indicating the microscopic details we have included are good approximations.

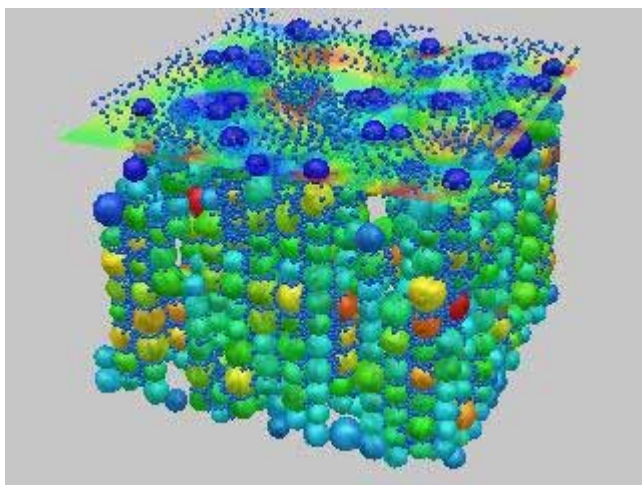


Figure 11 Simulation cell for magnetic brush. Charge flow and electric fields are complex during the development process.

Discussion and summary

The high resolution field probe has enabled us to look at the electrical properties of the magnetic brush in some detail. We have seen the average dielectric constant and conductivity vary as we move through the development zone as well as the variation in these quantities. We have also observed configurations which have lower variation in conductivity over the development zone produce lower noise in the developed image.

The notion of an average dielectric constant and conductivity characterizing a magnetic brush is very useful for understanding the first order behavior of development. However, when details of the developed image are on the scale of the structure of the magnetic brush and the time scales for development are comparable to the times these fluctuations persist, we will see noise in the image. The high resolution field probe can give us some insight into the source of this noise. We are coming to regard the distribution of the electrical properties of the magnetic brush as an important element in our understanding of the noise present in xerographic images. It is very encouraging that the particle simulations which rely on physically reasonable parameters give very reasonable results when compared to our field probe experiments. We look to both tools for guidance in improving magnetic brush development systems.

References:

- [1] L.B. Schien, Electrophotography and Development Physics, 2nd Edition, Springer Verlag, 1992.
- [2] J.J. Folkins, Intermediate conductivities- The crossover function for insulative and conductive two-component magnetic brush development in electrophotography, IEEE Trans. Ind. Appl. Vol 24, 1988
- [3] Jack LeStrange and Dan Hays private communication
- [4] D. M. Pai and B. E. Springett "Physics of electrophotography" Rev. Mod. Phys. 65, pp 163 - 211 (1993)

- [5] J. G. Shaw, A. T. Retzlaff, Proc. 20th Ann. Meeting Adhesion Soc., ed. L. Drzal and H. Schreiber (Blackburg, VA: Adhesion Soc. 1997) p223
- [6] A. T. Retzlaff, J. G. Shaw "Simulation of Multi-component Charged Particle Systems" Fall Proceedings Materials Research Society, Volume 759 (2002)

Acknowledgement

We want to thank Bill Wayman, Dan Hays, and Ted Retzlaff for their invaluable assistance with this work

Author Biography

Michael Thompson is a member of the research staff at the Xerox Research Center Webster where he has worked in various areas of xerographic process physics since 1980. He has a PhD in theoretical condensed matter physics and holds patents in the areas of single and dual component xerographic marking, novel marking processes, control of xerographic systems and MICR.